Fundamental Limits in Cellular Networks with Point Process Partial Area Statistics

Lélio Chetot[1], Jean-Marie Gorce[1], Jean-Marc Kélif[2]

[1]Univ Lyon, INSA Lyon, Inria, CITI, F-69621 Villeurbanne, France. [2]Orange Labs, Châtillon, France.

Abstract—**Despite the huge number of contributions dealing with the evaluation of cellular networks performance, tackling with more and more complex systems including multi-tier networks or MIMO systems, the fundamental limits in terms of capacity in an information theory sense is not known for these networks. Stochastic geometry helped doing a step forward, relying on Palm theory and providing coverage statistic at the network scale. However, this statistic is not sufficient to establish a fundamental limit, namely to characterise a Shannon capacity region of the network. In this paper, we propose a new approach exploiting the cell capacity of the Spatial Continuum Broadcast Channel (SCBC) recently introduced for an isolated cell. The network capacity is linked to the cells' geometry statistics in a Voronoi tessellation. The fundamental limit is characterised by the minimal average cell power required in a network modelled as a Point Process (PP) to achieve a desired rate distribution. A direct relation is established between this minimum average power and the partial area statistics of the cells geometry, which constitute a sufficient statistic. Our approach is validated through Monte-Carlo simulations.**

Index Terms—**Cellular networks, Voronoi tessellation, Point Processes, Stochastic geometry, NOMA, Fundamental limit.**

I. Introduction

A. Motivation and related work

Stochastic geometry has been widely used for cellular network performance evaluation since [1] and pioneering work in wireless ad-hoc networks in [2, 3]. It provides a means of evaluating in a simple manner the overall performance in a cellular network from the local statistic around a reference point and under the assumption of spatial stationarity. Most of the literature published beyond [1], see [4] for a recent overview, derive analytic results from the coverage statistic. Despite the relative simplicity of the underlying propagation models, the coverage statistic appeared to fit quite well with real measurements [5]. However, this coverage statistic does not includes the impact of cell's load on joint rates. This cell load is studied as a function of the Base Stations (BSs) activity probability in [6, 7] and over a two-tier Poisson Point Process (PPP) network in [8]. This cell load – defined as the product of the mean packet size, the users density and the cell area – is a good approximation of the sum-rate but does not consider the relation between rates and radio link quality. This relation is introduced in [9] for a noisy limited network but relies explicitly on an orthogonal resource sharing strategy inside each cell. In [10], the load in a single cell in the uplink is formalised through the joint transmissions probability and considering successive interference cancellation (SIC) but the approach was not generalised to a multi-cell scenario.

None of the aforementioned results provide a fundamental limit in the meaning of Shannon theory [11]. Remind that for a point-to-point (P2P) channel, the Shannon capacity establishes the maximal rate at which an information can be sent with an arbitrarily low error probability when the coding block length tends to infinity. The capacity thus represents a fundamental limit that cannot be over-passed.

Evaluating an analogous result of the Shannon capacity for a cellular network is the objective of this paper, under some specific conditions. Following the model of [9], we consider a noisy limited network. In our case, each cell is assimilated to a Gaussian memoryless broadcast channel (BC). Its capacity region is known and achievable with a superposition coding (SC) strategy [12]. This gives rise to the unprecedented interest for Non Orthogonal Multiple Access (NOMA) techniques for 5G networks. Considering the BC model in a multi-cell network is the core contribution of our paper.

Our approach relies on the characterization of the distribution of cell's geometry. The cell area statistics have been investigated in the general framework of Poisson Voronoi cells in [13, 14] and empirical models based on fitting a generalised gamma distribution have been obtained. We will show below that this statistic is not sufficient in our case and additional knowledge is required.

B. Contributions and outcomes

The goal of this paper is to characterise the Shannon capacity region of a noisy limited cellular network

Over the years, the P2P Shannon capacity theorem has been extended to multi-user scenarios by Shannon himself and others [12], through the definition of a capacity region. Given a typical K-user scenario , e.g. the K-user BC, the capacity region is characterised by the set of joint rates which are simultaneously feasible. In Shannon's wording, the rates $(R_1, R_2, \ldots, R_k)$ are feasible if there exist a joint encoding-scheduling strategy such that the transmission error probability tends to 0 when the coding length tends to infinity. Note that this coding length is usually measured in numbers of channel uses ($c.u.$), and can be thought as a number of resource elements used for a packet transmission.

The BC is a good abstraction for a radio-cell with K mobile nodes in the downlink and is used in [15] to establish the capacity region of a cell with a discrete set of nodes. It is shown that a classical orthogonal resource sharing (e.g. TDMA or FDMA) is not optimal for a large class of physical channels, and gives rise to NOMA techniques. For Gaussian channels

(under Additive White Gaussian noise (AWGN)), the capacity region is known and any point in this region is achievable with superposition coding (SC) [12].

The Shannon capacity region of the Gaussian BC was reformulated for a random distribution of users with the continuum model, denoted SCBC in [16] to take into account a distribution of nodes instead of a discrete set of nodes. A SCBC is fully characterised by a cell geometry and a probability density function $\rho(x)$, with $x \in C$ and where C is the cell. $\rho(x)$ is called the rate distribution of the cell, and stands for the spatial random distribution of downlink rate requests.

Definition I.1. *A rate distribution $\rho(x)$ is said achievable under some power constraint, if a joint transmission scheme exists such that the error transmission tends to 0 for all users when the number of channel uses tends to infinity.*

The SCBC Shannon capacity region is called the access capacity region. The definition follows:

Definition I.2. *The power constrained SCBC access capacity region of a cell is the set of feasible rate densities $\rho(x)$ for a given power granted to the BS.*

This access capacity region has been analysed in [17], for a single isolated cell with regular pathloss and shadowing, through its alternative form, the fundamental energy efficiency-spectral efficiency (EE-SE) trade-off (see sec. II-A for details). At the network scale, this access capacity region can be defined similarly and should characterise the set of feasible rate distributions at the network scale. Unfortunately, such an extension is not straightforward since it relies on high order statistics of the cell's geometry distribution in terms of area and shape.

The aim of this paper is therefore to explore the relation between the cell geometry distribution and the EE-SE trade-off. It is worth mentioning that the following assumptions are made for mathematical tractability purpose :

- Fast fading, static fading and shadowing are not explicitly considered in this model[1].
- Single antennas are only considered at both transmitters and receivers. Considering multi-antenna BSs under perfect channel state information at the transmitter (CSIT) is straitghforward but has been discarded due to the lack of space.
- Interference between cells is not considered since this paper focuses on the impact of the cell's geometry. The extension to interfering cells is still an open problem.

It is true that these assumptions simplify the derivation of the network fundamental limits and may lack of realism. Nevertheless, we believe that this model is a fundamental key model of a cellular network, playing a similar role as the Gaussian channel for a P2P transmission. The resulting

---

[1]In [18], any network (even an hexagonal lattice) with shadowing was shown to be equivalent to a PP network without shadowing. This is true for first order statistics, but not for higher order statistics as herein required.

Shannon P2P capacity ($\log_2(1 + SNR)$) deserved to be known despite its simplicity.

The main results of this paper are as follows. In Theorem 1, the fundamental EE-SE limit is established under the assumptions mentioned above. The expression of the minimal average power required for a given rate spatial distribution from [16] is extended at the network scale. In Theorem 2, a direct relationship is established between this average minimal cell power and a sufficient statistic of the underlying PP through the area and partial area distributions, defined in Sec.II-C. These distributions characterise the high order statistics of the cellular network. This theorem is evaluated by extensive simulations giving credit to the proposed formulation. The price of randomness (in terms of transmission power excess) is computed and analysed by confronting PPP and Matérn Point Process (MPP) networks.

II. MODELS AND BACKGROUND

The cellular network is modelled with two PPs. One stands for the BSs and the other for the node requests. The latter is modelled with a PPP of density λ_T and lead to a uniform spatial distribution of nodes. For the sake of simplicity, it is assumed that each BS aims at transmitting non correlated and independent information to its nodes with a fixed amount of information per packet denoted I_0. The rate spatial distribution is therefore uniformand given by $\rho_0 = \lambda_T I_0$ expressed in nat.cu^{-1}.m^{-2}, where *cu* stands for *channel use*. Each node is associated to its nearest BS.

Let us consider a cell C of area $|C| = A$. Its average spectral efficiency is $\eta = A\rho_0$. Given a reference time T, the BS has to serve a random selection of nodes (the sum rate is in average $TA\rho_0$), picked up randomly over the cell. For a given selection of users, the $K-$user Gaussian BC is appropriate and has a known capacity region [12], but this model does not capture the users randomness.

A. Fundamental limit in a single cell

For the sake of completeness, this section summarises the results from [16]. For each node k the received signal is $y_k = x_k + z_k$, where x_k is the signal transmitted by the BS, and z_k an equivalent noise of variance $v_k = N_0/l_k$ where $l_k = l(r_k)$ is a continuously decreasing pathloss function and r_k the BS-node distance associated to the kth node. v_k is call the equivalent noise power in the rest of this paper. Hence, the SNR at the receiver is given by $\gamma_k := P_k/v_k$ where P_k is the power dedicated to the kth node. Each radio link considered individually corresponds to a Gaussian P2P channel subject to an average power constraint. Its fundamental limit is given by the maximal spectral efficiency per channel use $\eta_k = 0.5 \log(1 + \gamma_k)$ in nat.cu^{-1}. Alternatively, the minimal power density required to achieve a given spectral efficiency is

$$P_{min} = (e^{2\eta} - 1)N_0, \qquad (1)$$

where N_0 is the receiver noise power density.

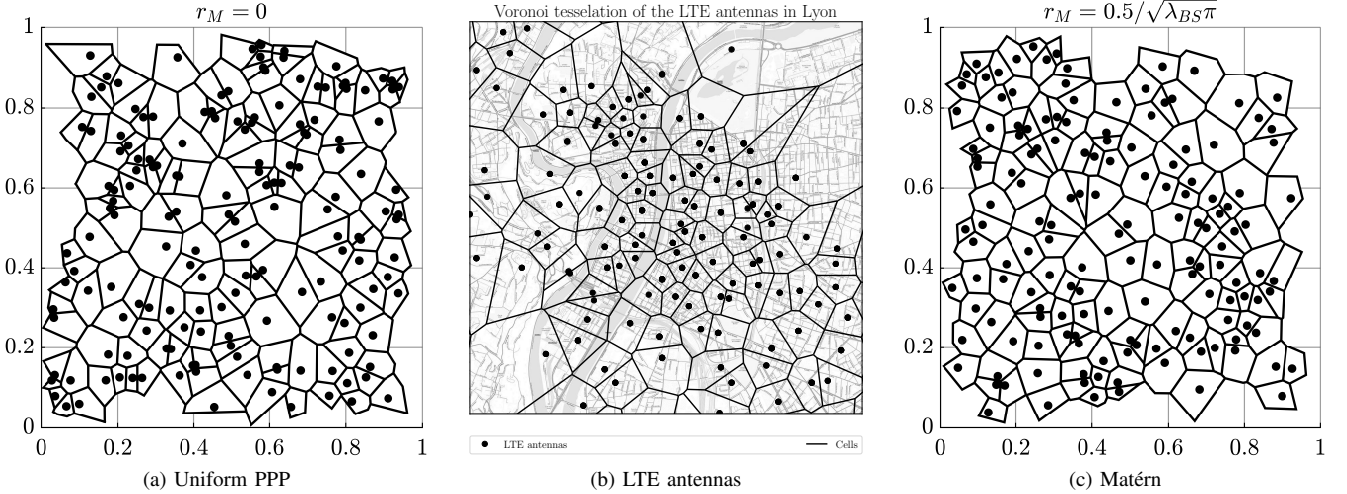The joint fundamental limit of the $k-$user BC, when the individual rates are all equal and where each node requires

Fig. 1. Three Voronoi tessellations corresponding to a PPP **(a)**, the LTE antennas of the city of Lyon **(b)** and a MPP **(c)** (Matérn hard-core type II point process). Both PPP and MPP have the same density $\lambda_P = \lambda_M = 200$. The cells in periphery of the Voronoi tessellation of the LTE antennas may be much larger than the average since we did not take into account the antennas of the adjacent cities.

the same SINR γ^* is known and achievable with SC [12]. The minimal power required at the BS is the sum of all individual powers $P_{sum} = \sum_{k=1}^{K} P_k$, where the nodes are ordered from the nearest to the farthest point and where the individual powers are

$$P_k = \gamma^* \cdot \left(\nu_k + \sum_{i=1}^{k-1} P_i \right). \tag{2}$$

The additional terms in P_k stand for the intra-cell interference due to SC, while the terms for $i > k$ are cancelled with successive decoding. Relying on this fundamental limit in a Gaussian BC, we computed in [16] the minimal power in a single isolated cell, taking the limit when $T \rightarrow \infty$, corresponding to the Shannon asymptotic regime for the SCBC.

Let us define the cumulative density function (cdf) $F(\nu)$ representing the sum-rate associated to all nodes with an equivalent noise lower than ν, and let $G(\nu)$ and $f(\nu)$ be respectively the corresponding complementary cumulative density function (ccdf) and the probability density function (pdf).

By taking the limit $T \rightarrow \infty$, the minimal transmission power per channel use for the nth cell was established as:

$$P_{min,n} = 2\eta_n \cdot \int_0^{\nu_{max}} \nu(\nu) \cdot e^{2\eta_n \cdot G(\nu)} d\nu, \tag{3}$$

where ν_{max} is the maximum equivalent noise, holding at the cell edge. Note that static fading and shadowing can be integrated in this model by computing an appropriate distribution of $f(\nu)$.

Eq(3) characterises the fundamental EE-SE limits of this cell by providing a lower bound on the minimum average power required to achieve any desired rate distribution. It relies on the cell properties (through $f(\nu)$ and $G(\nu)$) and on the sum-rate requirement, i.e. η_n. The attention of the reader is drawn to the fact that this bound is only achievable with SC and establishes a fundamental limit of a NOMA strategy.

This result is the keystone element used below to assess the fundamental limit at the network scale.

B. Network elements

The network is modelled as a Voronoi tessellation derived from a random PP of BSs with density λ. The Voronoi cell associated to a BS is the set of closest points. More formally, Φ_{BS} denotes the set of all BSs. Let $z \in \Phi_{BS}$ be a BS of the PP. Its Voronoi cell $C(z)$ is defined by

$$C(z) := \{x \in \mathbb{R}^2 : \forall z' \in \Phi_{BS} \backslash \{z\}, \ \|z - x\| < \|z' - x\|\}. \tag{4}$$

The set of all the Voronoi cells forms the Voronoi tessellation of the network as represented in fig. 1a for a uniform PPP.

This model based on a uniform random distribution of BSs may not well describe a physical cellular network where the BSs locations are partly correlated [3, 19]. For instance, see fig. 1b for the Voronoi tessellation of the LTE antennas in Lyon for the ISP Orange (according to the French National Frequencies Agency data [20]). The Matérn Point Process (MPP) is a modified model allowing to take into account spatial correlations [21, 3]. In the rest of this paper, we will consider the Matérn Hard-Core Process of type II defined in [3]. Given r_M the Matérn radius corresponding to the minimal distance, a MPP is obtained through the following steps:

1. Generate the parent PPP $\Phi_P = \{x_i\}$ with density λ_P.
2. Give random marks $\{m_i \mid m_i \sim \mathcal{U}([0,1])\}$ to each point $x_i \in \Phi_P$ where $\mathcal{U}([0,1])$ denotes the uniform probability law in the range $[0,1]$.
3. For each $x_i \in \Phi_P$:
   i. For each $x_j \in \Phi_P$ with $j \neq i$, if $m_j < m_i$ and $\|x_i - x_j\| < r_M$, add the mark ($\triangle$) to x_j
4. Form a new point process Φ_M with the x_i without the mark ($\triangle$). In other words, $\Phi_M = \Phi_P \backslash \{x_i \text{ with the mark } (\triangle)\}$.

The new process Φ_M is a MPP with density λ_M given by

$$\lambda_M = \frac{1 - \exp\left(-\lambda_P \pi r_M^2\right)}{\pi r_M^2}. \tag{5}$$

An MPP, as in fig. 1c, can be easily generated from a PPP, with a known density and providing more regular cells.

C. A sufficient statistic for cells geometry

The geometry (cell size and shape) impacts the fundamental limit of the network. But, as shown in section III, the cells areas and partial areas are a sufficient statistic. Considering a single BS located in z and its Voronoi cell $C(z)$, the total area and two partial area measures as functions of a distance $r > 0$ as represented in fig. 2 are defined.

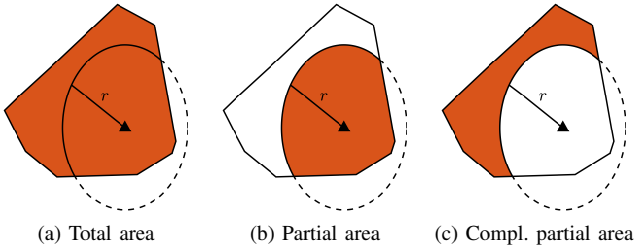(a) Total area   (b) Partial area   (c) Compl. partial area

Fig. 2. The total area of a cell associated to a BS (black triangle) is represented in (a). For a given distance r, the partial and complementary partial areas are represented in (b) and (c) respectively.

1) *Total area:* $A := |C(z)|$, where $|S|$ denotes the cardinal of the set S.

2) *Partial area (PA):* The partial area is $A(r) := |\{x \in C(z) : \|z - x\| \leq r\}|$.

3) *Complementary partial area (CPA):* The complementary partial area is $A_c(r) := |\{x \in C(z) : \|z - x\| > r\}|$.

In a PP network, these areas are random variables parametrised by λ and thus noted A_λ, $A_\lambda(r)$ and $A_{c,\lambda}(r)$. For a normalised PP i.e. with a density $\lambda = 1$, the corresponding variables are noted A, $A(r)$ and $A_c(r)$. We denote further the moment generating function (MGF) of the CPA by:

$$\mathcal{M}_{A_{c,\lambda}(r)}(t) := \sum_{k=0}^{+\infty} \frac{t^k \mathbb{E}\left[A_{c,\lambda}(r)^k\right]}{k!}. \tag{6}$$

Thanks to the scaling properties of the MGF, the following relation between the CPA's MGFs for a non normalised and normalised PP holds:

$$\mathcal{M}_{A_{\lambda,c}(r)}(t) = \mathcal{M}_{A_c(u)}\left(\frac{t}{\lambda}\right), \tag{7}$$

where $u := \sqrt{\lambda} r$ is a normalised distance.

III. Minimum Transmission Power in PP Networks

A. AMCP derivation

Let us introduce the partial sum-rate of the nth cell $R_n(\nu) := 2\eta_n F_n(\nu)$ which corresponds to the sum-rate of nodes with an equivalent noise lower than ν. The differential sum-rate associated to C_n with respect to ν is then given by:

$$dR_n(\nu) = 2\eta_n f_n(\nu)d\nu. \tag{8}$$

The complementary partial sum-rate, associated to the nodes with an equivalent noise greater than or equal to ν is:

$$R_{c,n}(\nu) = 2\eta_n G_n(\nu). \tag{9}$$

With these definitions, the AMCP expression follows:

Theorem 1 (Average minimal cell power – AMCP)**.** *The average minimal cell power in a PP network is*

$$AMCP = \int_0^{\nu_{max}} \left(\mathbb{E}^0\left[e^{R_c(\nu)}\right] - 1\right) d\nu, \tag{10}$$

where $\mathbb{E}^0[\cdot]$ denotes the expectation for the Palm theory [2].

Proof. We can rewrite (3) using (8) and (9) as:

$$P_{min,n} = -\int_0^{\nu_{max}} \nu dR_n(\nu) e^{R_{c,n}(\nu)} d\nu \tag{11}$$

$$\overset{(i)}{=} -\nu_{max} + \int_0^{\nu_{max}} e^{R_{c,n}(\nu)} d\nu, \tag{12}$$

where (i) uses partial integration. AMCP is then given by:

$$AMCP = \mathbb{E}_n\left[P_{min,n}\right] \overset{(i)}{=} \mathbb{E}^0\left[P_{min,0}\right], \tag{13}$$

where (i) derives from Slivnyak's theorem (see [2]). Finally, by linearity of the expectation, AMCP is given by:

$$AMCP = -\nu_{max} + \int_0^{\nu_{max}} \mathbb{E}^0\left[e^{R_{c,0}(\nu)}\right] d\nu, \tag{14}$$

which straightforwardly leads to the result by denoting $R_c(\nu) := R_{c,0}(\nu)$ since the PP is uniform. $\square$

Using the CPA definition (section II), it comes:

Theorem 2 (AMCP w.r.t. CPA)**.** *The average minimal cell power in a PP network with a homogeneous rate distribution ρ_0 and a continuously decreasing pathloss function $l(r)$, is given by:*

$$AMCP = \int_0^{u_{max}} \nu'\left(\frac{u}{\sqrt{\lambda}}\right)\left(\mathcal{M}_{A_c(u)}(2\eta) - 1\right) du, \tag{15}$$

where $\nu'(u/\sqrt{\lambda}) = N_0 \frac{d}{du} l\left(u/\sqrt{\lambda}\right)^{-1}$ and u_{max} is the normalised coverage radius associated to ν_{max}. $\mathcal{M}_{A_c(u)}(.)$ is defined in section II-B.

Proof. By introducing the MGF of the complementary partial sum-rate given by

$$\mathcal{M}_{R_c(\nu)}(t) = \mathbb{E}\left[e^{tR_c(\nu)}\right] \tag{16}$$

one can rewrite (10) as

$$AMCP = \int_0^{\nu_{max}} \left(\mathcal{M}_{R_c(\nu)}(1) - 1\right) d\nu. \tag{17}$$

According to the assumptions (uniform rate and pathloss function), one have $R_c(\nu) = 2\rho_0 A_c(r(\nu))$ where $A_c(r)$ denotes the random variable of CPA defined in section II-C. Reminding that $u = \sqrt{\lambda} r$ is a normalised radius, one obtains:

$$\mathcal{M}_{R_c(\nu)}(1) \overset{(i)}{=} \mathcal{M}_{A_{\lambda,c}(r(\nu))}(2\rho_0) \overset{(ii)}{=} \mathcal{M}_{A_c(u)}\left(\frac{2\rho_0}{\lambda}\right), \tag{18}$$

where (i) and (ii) are obtained thanks to the scaling property of the MGF. The right hand term in (18) reveals a MGFs belonging to $\left\{ \mathcal{M}_{\tilde{A}_c(u)}(t) ; \forall u > 0, t > 0 \right\}$ independent of the operational parameters (λ, $l(r)$, η...) except through its arguments (u, t). Moreover, the quantity ρ_0/λ is nothing but the cell spectral efficiency η. Now, using (18) and rewriting (17) in terms of the normalised coverage radius u gives the result. $\quad\square$

When u increases, CPA decreases and so the non-zero CPA probability. For some large values of u, $A_c(u)$ exhibits a discontinuity on 0, with a peak. To overcome this, we use a Bernoulli random variable $b(u) \sim \mathcal{B}(\beta(u))$ defined as

$$b(u) = \begin{cases} 0 & \text{if } u \geq u_{max} \text{ with probability } 1 - \beta(u) \\ 1 & \text{if } u < u_{max} \text{ with probability } \beta(u) \end{cases} \quad (19)$$

where $\mathcal{B}(\cdot)$ denotes the Bernoulli probability law and $\beta(u)$ the probability of non-zero CPA for a given u. Hence, the random variable of the CPA can be written as

$$A_c(u) = b(u) \cdot \tilde{A}_c(u), \quad (20)$$

where $\tilde{A}_c(u)$ stands for the non-zero CPA. This refinement allows us to rewrite the MGF of the normalised CPA as

$$\mathcal{M}_{A_c(u)}(t) = (1 - \beta(u)) + \beta(u) \cdot \mathcal{M}_{\tilde{A}_c(u)}(t), \quad (21)$$

where the remaining MGF deals only with non-zero areas. The final expression of the AMCP is:

$$AMCP = \int_0^{u_{max}} \nu'\left(\frac{u}{\sqrt{\lambda}}\right) \beta(u) \left(\mathcal{M}_{\tilde{A}_c(u)}(2\eta) - 1 \right) du \quad (22)$$

Computing (22) requires the knowledge, for $u \in [0, u_{max}]$, of $\beta(u)$ and $\mathcal{M}_{\tilde{A}_c(u)}(t)$. We draw the attention of the reader that these laws are independent of the physical parameters and depend only on the PP kind. They can therefore be evaluated at once for each kind of PP. The physical parameters required in a second step to compute the integral in (22) are the maximal distance u_{max} over all the cells, the equivalent noise distribution $\nu(u)$ which depends on the pathloss function, the BS density λ and the desired spectral efficiency η.

B. CPA Moment-generating function

This section is dedicated to the study of the CPA's MGF. We address the problem of its convergence radius in III-B1 and its computation in III-B2.

1) Convergence radius: Let start with the remark that, for any $k \in \mathbb{N}$ and for $0 \leq u_1 \leq u_2$, the following inequality holds:

$$\mathbb{E}\left[(A_c(u_1))^k \right] \geq \mathbb{E}\left[(A_c(u_2))^k \right]. \quad (23)$$

Because the greater the coverage radius, the lower the CPA, so are its moments. The MGF inequality follows from (23),

$$\forall t > 0, \ \mathcal{M}_{A_c(u_1)}(t) \geq \mathcal{M}_{A_c(u_2)}(t) \quad (24)$$

and in particular with $u_1 = 0$ and $u_2 = u > 0$, we have

$$\forall t > 0, \ \mathcal{M}_{A_c(0)}(t) > \mathcal{M}_{A_c(u)}(t). \quad (25)$$

We denote $\varrho_c(u)$ the convergence radius of CPA's MGF for the coverage radius u. The MGF inequality (25) gives the following inequality between the convergence radii

$$\forall u > 0, \ \varrho_c(0) < \varrho_c(u). \quad (26)$$

Since (22) must be finite, the choice of 2η is bounded by the minimum convergence radius over the integration interval:

$$2\eta \leq \min_{u \in [0, u_{max}]} \varrho_c(u) = \varrho_c(0). \quad (27)$$

In order to find the value of $\varrho_c(0)$, we focus on the pdf of CPA for $u = 0$ which corresponds to the pdf of the Total Areas. In [13], the pdf of the total areas is well approximated by the *generalised gamma* ($G\Gamma$) probability law whose pdf is

$$f(x|a, p, d) = \frac{p}{a^d \Gamma\left(\frac{d}{p}\right)} x^{d-1} \exp\left(-\left(\frac{x}{a}\right)^p\right) \quad (28)$$

where a, p, d are positive parameters and $\Gamma(x) = \int_0^{+\infty} t^{x-1} e^{-x} dx$ denotes the gamma function.

Theorem 3 (Convergence radius of CPA's MGF)**.** *The convergence radius of $\mathcal{M}_{A_c(0)}(t)$ is given by*

$$\varrho_c^* = \begin{cases} 0 & \text{if } p < 1 \\ \frac{1}{a} & \text{if } p = 1 \\ +\infty & \text{if } p > 1 \end{cases} \quad (29)$$

Proof. The proof is given in Appendix A. $\quad\square$

It means that if $p > 1$, $\mathcal{M}_{A_c(0)}(t)$ converges for any t, and if $p = 1$, it converges for $t < a^{-1}$. For $p < 1$, the $\mathcal{M}_{A_c(0)}(t)$ diverges.

2) Computation: Let $\{x_i\}_{i=1,...,N}$ be a set of observed CPAs.

An empirical method is used to compute its MGF and consists in computing, for a real t, the mean of the set $\{e^{t x_i}\}_{i=1,...,N}$. The unbiased estimated MGF is then

$$\hat{\mathcal{M}}_{A_c(u)}(t) = \frac{1}{N} \sum_{i=1}^{N} e^{t x_i}. \quad (30)$$

IV. VALIDATION BY SIMULATIONS

Computing (22) and by extension (30) requires extensive Monte-Carlo simulations. The two algorithms used to simulate PP networks and to compute AMCP are now described.

The first one computes the Monte-Carlo Average Cell Power (MCMCP) by extensive simulations of real networks. It is done by generating N_{net} networks i.e. sets of BSs according a PPP with density λ_{BS} in a square region $\mathcal{R}$ of side D. For each network, N_T sets of nodes are generated. The average cell power of the individual networks are computed by averaging over all the powers required by the cells. Then, the MCMCP is obtained by averaging over all the individual average cell powers.

The second algorithm computes for $u \in [0, u_{max}]$ the estimated mgfs (see (30)) and ratios ($\hat{\beta}_u$) of non-zero CPAs. This corresponds to the case of a normalised PPP ($\lambda_{BS} = 1$)

(a) **Total areas – Left:** Uniform PPP, **Right:** Matérn PP (b) **CPA – Left:** Uniform PPP, **Right:** Matérn PP
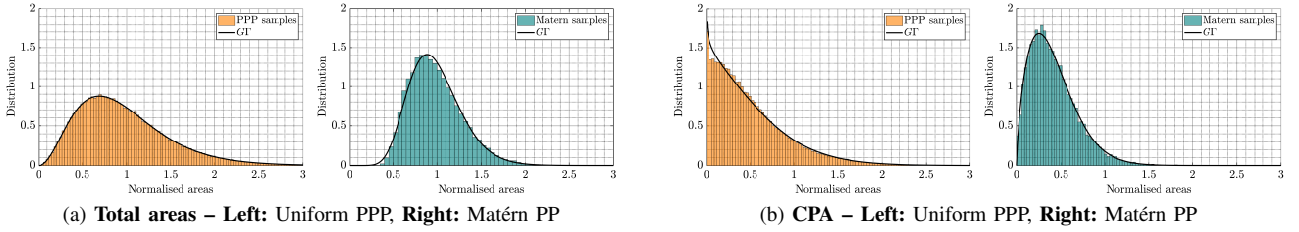
Fig. 3. Histograms and generalised gamma fits for cell total area distributions (a) and non-zero CPA distributions with $u = 0.8/\sqrt{\pi}$ (b).

that we will refer hereafter as the reference case. Once both the mgfs and ratios have been computed in the reference case, it is easy to use these results to compute the AMCPs of PPP with different BS densities $\lambda_{BS} \neq 1$. Indeed, (22) is a general expression that can be computed for any λ. One must simply pay attention that η depends on λ_{BS} since $\eta = \rho_0/\lambda_{BS}$.

Since the AMCP is the average power required by a cell to satisfy a continuum of users, it does not depend on the users density λ_T and only needs to be computed once. Furthermore, there is no need of new simulations when the parameters of the network change. Finally, the computation of the AMCP for a PPP with density $\lambda_{BS} \neq 1$ reduces to a simple integral calculation which takes considerably less time than a complete simulation. In practice, computing the average cell power with the first algorithm for only one value of λ_T requires approximately the same simulation time as computing the AMCP for a range of λ_T. The time saved to assess the performance bound of a network is very significant. Hence, our algorithm allows to evaluate easily different network scenarios just by tuning the physical parameters. The comparison of the two average minimum powers is performed and AMCP is exploited to draw some conclusions on the energy performance in PP networks.

A. Monte-Carlo cell power simulations

The algorithm for computing the Monte-Carlo average cell power (MCACP) simulator is the following:

1. Compute the region area $A_{\mathcal{R}} = D^2$.
2. For $i = 1, \ldots, N_{net}$:
    i. Draw the number n_{BS} according to a Poisson law with parameter $A_{\mathcal{R}} \times \lambda_{BS}$.
    ii. Generate a network $\mathcal{N}_i$ with n_{BS} BSs whose positions are drawn uniformly in $\mathcal{R}$.
    iii. For $j = 1, \ldots, N_T$:
        a. Draw the number n_T according to a Poisson law with parameter $A_{\mathcal{R}} \times \lambda_T$.
        b. Generate n_T nodes in the network $\mathcal{N}_i$ whose positions are drawn uniformly in $\mathcal{R}$ and associate each of them to the nearest BS.
        c. Compute the power P_j required by each cell in $\mathcal{N}_i$.
    iv. Compute the network's average cell power required by $\mathcal{N}_i$ such as $P_i = \sum_{j=1}^{N_T} P_j/N_T$.
3. Compute the MCACP $\hat{\bar{P}} = \sum_{i=1}^{N_{net}} P_i/N_{net}$

B. MGF and non-zero CPAs ratios based simulator

The algorithm for computing the estimated mgf (30) and non-zero CPAs ratios $\hat{\beta}_u$ is the following:

1. Initialize empty lists $\mathcal{L}_u$ for each $u \in \mathbf{u}$.
2. Compute the region area $A_{\mathcal{R}} = D^2$.
3. For $i = 1, \ldots, N_{net}$:
    i. Draw the number n_{BS} according to a Poisson law with parameter $A_{\mathcal{R}} \times \lambda_{BS}$.
    ii. Generate a network $\mathcal{N}_i$ with n_{BS} BSs whose positions are drawn uniformly in $\mathcal{R}$.
    iii. Build the Voronoi tessellation of the $\mathcal{N}_i$'s BSs.
    iv. For $u \in \mathbf{u}$, compute the CPAs of each cell in $\mathcal{N}$ for the coverage radius u and add them to the list $\mathcal{L}_u$.
4. Estimate the MGFs of the non-zero normalised CPA for each $u \in \mathbf{u}$: $\hat{\mathcal{M}}_u = \sum_{x \in \mathcal{L}_u} e^{\eta \lambda_{BS} x}/(N_{net} A_{\mathcal{R}} \lambda_{BS})$.
5. Estimate $\hat{\beta}_u$ of non-zero CPA for each $\mathcal{L}_u$.

V. Results

The cells' geometry statistic is evaluated for both PPP and MPP. The areas and CPA distributions as a function of the radius $u = r\sqrt{\lambda_{BS}} = r/(\sqrt{\pi}r_{avg})$ have been obtained. $r_{avg} := 1/\sqrt{\pi\lambda_{BS}}$ is the radius of a disk with its area equal to the average cell area. The distributions of the total areas and the CPAs are provided resp. in figs. 3a and 3b, as well as the best $G\Gamma$ fit. For PPP, our results are similar to those from [13] with ($a = 0.315, p = 1.04, d = 3.3$). According to Th.3, the convergence radius is infinite, meaning that AMCP is always finite whatever the network load. However, since p is close to 1, for which the convergence radius is lower bounded by a^{-1}, it may be interesting to compute the corresponding limit, with $a = 0.315$, leading to $\eta = 2.32$bits.cu^{-1}, which has an interesting meaning as seen below in fig. 5.

For MPP, the parameters of the best $G\Gamma$ fitting are ($a = 0.04, p = 0.85, b = 12.9$) and seem to indicate that the mgf diverges according to Th.3. However, this fit is loose and artificially increases the probability of high values, compared to the empirical values. Simulation results in terms of minimum power are provided in figs. 4 and 5. They have been obtained for the parameters given in table I. To facilitate the interpretation, spectral efficiency values are given in this section in bits.cu^{-1} using $\eta_{nat} = \eta_{bits} \times \ln 2$.

Choosing N_{net} and N_T as large as possible to obtain more accurate results is necessary but is limited by the computational time. Choosing a large N_{net} appears more important
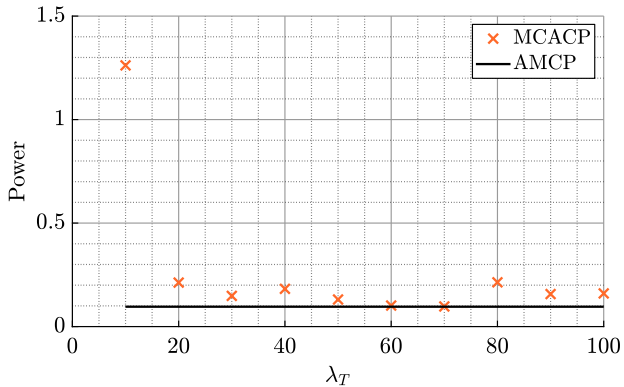
Fig. 4. Comparison between the MCACP and the AMCP. When the node density increases, the MCACP tends to the AMCP.

Fig. 5. Confrontation of the PPP's AMCP, the Matérn's AMCP and the MCCP for different values of η and different pathlosses.

than choosing a large N_T especially when the nodes density λ_T is high enough.

TABLE I
PARAMETERS USED FOR THE RESULTS IN FIGS. 4 AND 5.

Parameter	Figure 4	Figure 5
$\mathcal{R}$	1×1	1×1
λ_{BS}	200	200
λ_T	$\{10, 20, s, 100\}$	$\varnothing$
η	2.1640 bits.cu^{-1}	$[0.0721, 4.4724]$ bits.cu^{-1}
N_0	1	1
α	2	$[2, 4]$
r_0	1	$0.01 \times r_{avg}$
$l(r)$	r^{-2}	$(r/r_0)^{-\alpha}$
$\mathbf{r}$	$\{0, 0.01, s, 3\} \times r_{avg}$	$\{0, 0.01, s, 3\} \times r_{avg}$
r_M	$\varnothing$	$0.9 \times r_{avg}$
N_{net}	1000	$\varnothing$
N_T	100	$\varnothing$

Figure 4 shows the convergence for a PPP network of the MCACP to the AMCP when the nodes density λ_T increases. The resulting MCACP decrease when λ_T grows since the SC encoding strategy improves, allowing to approach the AMCP fundamental limit, at least in the low SE regime. This validates the AMCP to be the power required by a continuum of users at the network scale. Note that for MCACP curve, the network sum-rate is kept constant ($\eta = 2.164$ bits.cu^{-1}), meaning that the increase of λ_T is always counterbalanced by a decrease in the individual rates. It is also worth mentioning that the proposed MCACP curve is not smooth despite a very large number of Monte-Carlo simulations (100 runs for each of 1000 random networks of 200 BS in average). These simulations reveal the distribution of cell areas in a PPP includes rare but very large cells consuming a high part of the network power. The reason is the exponential relation of the cell power with respect to the sum-rate as seen in (3).

Figure 5 confronts the PPP and MPP AMCPs as functions of η (x-axis) and for different pathloss strengths α (indexed by the colour bar on right). The comparison is also made w.r.t the Minimal Circular Cell Power (MCCP):

$$MCCP = -\nu(r_{avg}) + \int_0^{r_{avg}} \frac{d\nu(r)}{dr} e^{\eta \frac{\pi r^2}{\lambda_{BS}}} dr. \quad (31)$$
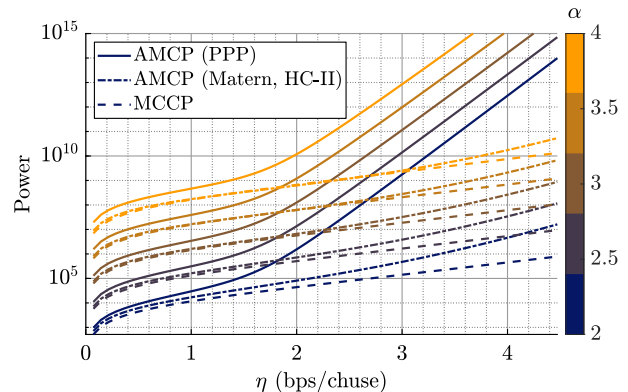
The MCCP is nothing but the AMCP applied to a single cell network with a circular shape and a radius $r = r_{avg}$, thus having its area equal to the average area (PPP model). The circular cell is an ideal case from a geometry point-of-view.

The gap between AMCP (plain curves) and MCCP (dashed lines) increases with both rate and pathloss. We clearly see around $\eta = 2$ bits.cu^{-1} a significant increase of the slope of the AMCP curve. This power overconsumption represents the price to be paid for the cells geometry randomness due to a pure random deployment. We also plot in the same figure the AMCP obtained with the MPP from section II, highlighting how the network randomness impacts the power efficiency. Since a MPP has a more regular CPA distribution, its AMCP is closer to the MCCP. Hence, the power penalty w.r.t. the ideal circular cell starts around 3bits.cu^{-1} with a lower slope.

These curves show the power saving an operator can get by optimising the cells distribution. From these results, we conjecture that a PPP does not behave as a real network at the second-order and beyond. A Matérn hard-core type II model is a good candidate for this, but need to be tuned to fit with experimental data.

VI. CONCLUSION

In this paper, we exploit the high order statistics of the radio links, through CPA distribution, from the newly established analytic relation between AMCP and CPA statistics. This result has been validated with Monte-Carlo simulations. The important result is how the cells geometry randomness in a PPP generates a huge power overconsumption in the network, which can be significantly reduced in a more regular network, as modelled with a MPP. Our theoretical tool can help engineers to balance their operational costs between the cost of randomness and the cost of optimization. At the best of our knowledge, this paper is the first contribution dealing with the fundamental limit of a cellular network, considering high order statistics in PPs.

APPENDIX A
PROOF OF THEOREM 3

The moments of a $G\Gamma$ distributed random variable X are:

$$\forall k \in \mathbb{N}, \ \mathbb{E}\left[X^k\right] = a^k \Gamma\left((d+k)p^{-1}\right) \Gamma\left(dp^{-1}\right)^{-1}. \quad (32)$$

By using the series expansion of the MGF from (16), one have

$$\mathcal{M}_{R_c(\nu)}(t) = \sum_{k=0}^{+\infty} \frac{t^k}{k!} \mathbb{E}\left[R_c(\nu)^k\right]. \quad (33)$$

Replacing (32) in (33), the CPA's MGF for $u = 0$ becomes

$$\mathcal{M}_{A_c(0)}(t) = \sum_{k=0}^{+\infty} \frac{t^k}{k!} a^k \Gamma\left((d+k)p^{-1}\right) \Gamma\left(dp^{-1}\right)^{-1}. \quad (34)$$

Let the sequences (v_k) and (w_k) be defined as

$$v_k = \frac{a^k}{k!} \Gamma\left((d+k)p^{-1}\right) \Gamma\left(dp^{-1}\right)^{-1} \quad , \quad w_k = v_k/v_{k-1}. \quad (35)$$

According to D'Alembert's rule, $1/\varrho_c^* = \lim_{k\to+\infty} w_k$, where:

$$w_k = ak^{-1} \Gamma\left((d+k)p^{-1}\right) \Gamma\left((d+k-1)p^{-1}\right)^{-1}. \quad (36)$$

Using the following property of the Γ-function:

$$\Gamma(x+y) = \Gamma(x)\Gamma(y)B(x,y)^{-1} \quad , \quad \forall x, y \in \mathbb{R}^+, \quad (37)$$

with $B(,)$ the Beta function, one obtain:

$$w_k = ak^{-1} \Gamma\left(p^{-1}\right) B\left((d+k-1)p^{-1}, p^{-1}\right)^{-1}. \quad (38)$$

The Stirling's approximation of the Beta function, given y

$$B(x,y) \underset{x\to+\infty}{\sim} \Gamma(y)x^{-y}, \quad (39)$$

used in (38), leads to

$$w_k \underset{k\to+\infty}{\sim} ak^{-1}\left(kp^{-1}\right)^{1/p}. \quad (40)$$

The value of $\varrho_c^* = 1/\lim_{k\to+\infty} w_k$ is obtained with (40)
- if $p < 1$ then $1/p - 1 > 0$ and $\varrho_c^* = 0$;
- if $p = 1$ then $1/p - 1 = 0$ and $\varrho_c^* = 1/a$;
- if $p > 1$ then $1/p - 1 < 0$ and $\varrho_c^* = +\infty$.

REFERENCES

[1] J. G. Andrews, F. Baccelli, and R. K. Ganti. "A tractable approach to coverage and rate in cellular networks". In: *IEEE Trans. Commun.* 59.11 (2011), pp. 3122–3134.

[2] F. Baccelli and S. Zuyev. "Stochastic geometry models of mobile communication networks". In: *Frontiers in queueing* (1997), pp. 227–243.

[3] M. Haenggi. *Stochastic geometry for wireless networks*. Cambridge University Press, 2012.

[4] H. ElSawy et al. "Modeling and analysis of cellular networks using stochastic geometry: A tutorial". In: *IEEE Comm. Surveys & Tutorials* 19.1 (2017), pp. 167–203.

[5] A. Guo and M. Haenggi. "Spatial stochastic models and metrics for the structure of base stations in cellular networks". In: *IEEE Trans. Wireless Commun.* 12.11 (2013), pp. 5800–5812.

[6] H. S. Dhillon, R. K. Ganti, and J. G. Andrews. "Load-aware modeling and analysis of heterogeneous cellular networks". In: *IEEE Trans. Wireless Commun.* 12.4 (2013), pp. 1666–1677.

[7] S. Lee and K. Huang. "Coverage and economy of cellular networks with many base stations". In: *IEEE Commun. Let.* 16.7 (2012), pp. 1038–1040.

[8] Y. J. Sang and K. S. Kim. "Load distribution in heterogeneous cellular networks". In: *IEEE Communications Letters* 18.2 (2014), pp. 237–240.

[9] G. Ghatak, A. De Domenico, and M. Coupechoux. "Accurate Characterization of Dynamic Cell Load in Noise-Limited Random Cellular Networks". In: *IEEE 88th Vehic. Tech. Conf. (VTC Fall)*. 2018.

[10] H. S. Dhillon et al. "Fundamentals of throughput maximization with random arrivals for M2M communications". In: *IEEE Transactions on Communications* 62.11 (2014), pp. 4094–4109.

[11] C. E. Shannon. "A mathematical theory of communication". In: *Bell syst. tech. journal* (1948), pp. 379–423.

[12] A. El Gamal and Y.-H. Kim. *Network information theory*. Cambridge university press, 2011.

[13] M. Tanemura. "Statistical distributions of Poisson Voronoi cells in two and three dimensions". In: *Forma* 18 (2003), pp. 221–247. ISSN: 0911-6036.

[14] J. Ferenc and Z. Néda. "On the size distribution of Poisson Voronoi cells". In: *Physica A: Statistical Mechanics and its Applications* 385.2 (2007), pp. 518–526.

[15] L. Li and A. J. Goldsmith. "Capacity and optimal resource allocation for fading broadcast channels. II. Outage capacity". In: *IEEE Trans. IT* 47.3 (2001), pp. 1103–1127.

[16] J.-M. Gorce, H. V. Poor, and J.-M. Kelif. "Spatial Continuum Model: Toward the Fundamental Limits of Dense Wireless Networks". In: *IEEE Globecom*. 2016.

[17] J.-M. Gorce et al. "Fundamental limits of a dense iot cell in the uplink". In: *IEEE WiOpt*. 2017.

[18] B. Błaszczyszyn, M. K. Karray, and H. P. Keeler. "Using Poisson processes to model lattice cellular networks". In: *IEEE Infocom*. 2013, pp. 773–781.

[19] N. Deng, W. Zhou, and M. Haenggi. "The Ginibre Point Process as a Model for Wireless Networks With Repulsion." In: *IEEE Trans. Wireless Commun.* 14.1 (2015), pp. 107–121.

[20] *Observatoire de l'Agence Nationale des Fréquences*. Visited on 3 Jan. 2019. URL: https://data.anfr.fr/anfr/.

[21] A. Busson, G. Chelius, and J.-M. Gorce. *Interference Modeling in CSMA Multi-Hop Wireless Networks*. Research Report RR-6624. INRIA, 2009, p. 21.